

SUPPORTING INFORMATION

Hydrogen evolution by cobalt hangman porphyrins under operating conditions studied by vibrational spectro-electrochemistry

Patrycja Kielbasa^{a/b}, Marius Horch^a, Pierre Wrzolek^c, Robert Goetz^d, Khoa H. Ly^e, Jacek Kozuch^f, Matthias Schwalbe^{c*} and Inez M. Weidinger^{d*}

Content:

Figure S1. SERR spectra of CoPCOOH immobilized via dip-coating on silver roughened electrodes at pH 10, measured at an applied potential of -1.5 V.

Figure S2. Catalytic response of CoPCOOH immobilized on silver roughened electrodes via dip-coating at pH 10.

Figure S3. Potential-dependent normalized intensity of the ν_4 band obtained from SERR spectra of CoPCOOH and CoPCOOMe physisorbed on silver roughened electrodes, measured at pH 4 and pH 10.

Figure S5. SERR spectra of (A) CoPCOOMe and (B) CoPCOOH immobilized on silver roughened electrodes, measured under open circuit conditions at pH 4. Dashed lines indicate positions of porphyrin vibrations.

Figure S6. Optimized structures and vibrational frequencies of CoTPP in the Co^{II} low-spin and Co^{I} high-spin / low-spin states, obtained by DFT calculations.

Figure S7. Absorption spectra of (A) CoPCOOH and (B) CoPCOOMe, dissolved in acetonitrile, in their (I) resting state and (II) after addition of the reductant KEt_3BH .

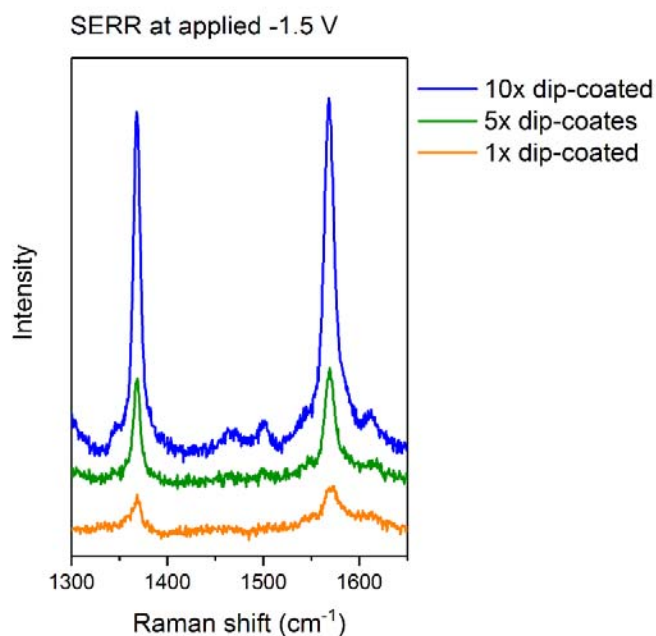


Figure S1. SERR spectra of CoPCOOH immobilized on silver roughened electrodes via dip-coating (orange: electrode dip-coated one time, green: electrode dip-coated five times, blue: electrode dip-coated ten times), measured at an applied potential of -1.5 V at pH 10. Each trace reflects an average of six spectra accumulated for 10 s with 600 μW laser power on the sample.

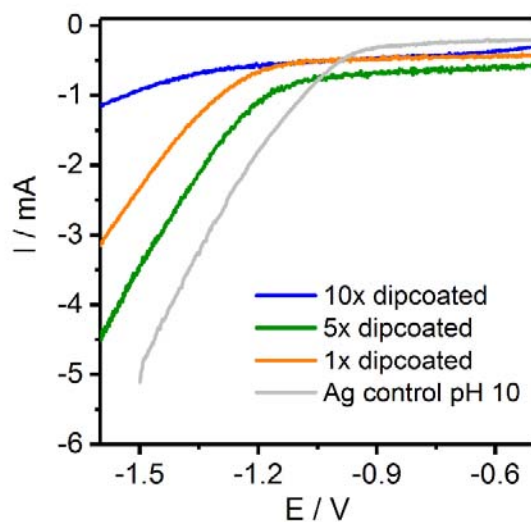


Figure S2. Catalytic currents measured with 5 mV/s scan rate at pH 10 from electrodes dip-coated one time (orange), five times (green), and ten times (blue) with CoPCOOH diluted in acetonitrile. The grey line corresponds to the catalytic current of the bare roughened silver electrode.

Increasing the number of dip-coating insertions of an electrode into a low-concentrated solution of CoPCOOH, the number of attached catalyst layers increases, as reflected by the intensities of the SERR spectra shown in Fig. S2. Increased amounts of compounds on the electrode surface also result in an increased catalytic activity (measured at pH 10) up to a certain amount (5 times dip-coated electrode), and then the catalytic current decreases (Fig. S1). For compounds dip-coated in highly concentrated solution, the catalytic activity is found to be lowest (Fig. 3). It seems that with higher amounts of catalysts on the surface, the activity of some layers is diminished by mass transport limitations, unfavourable packing, and/or lack of electrical contact.

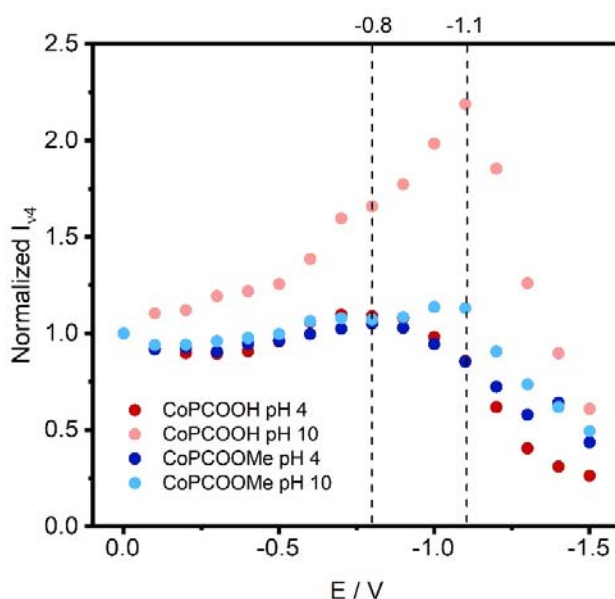


Figure S3. Potential-dependent normalized intensity of the ν_4 mode band obtained from SERR spectra of CoPCOOH and CoPCOOMe physisorbed on silver roughened electrodes, measured at pH 4 and pH 10. Intensities were normalized to the first spectrum obtained at open circuit or an applied potential of 0 V.

Plotting the normalized intensity of the ν_4 band from SERR spectro-electrochemistry experiments, turning point potentials of maximum intensity are observed. These potentials depend on pH (-1.1 V at pH 10 and -0.8 V at pH 4), but not on the type of compound. The observed values would fit to those reported for the pH-dependent potential of zero charge of silver.¹

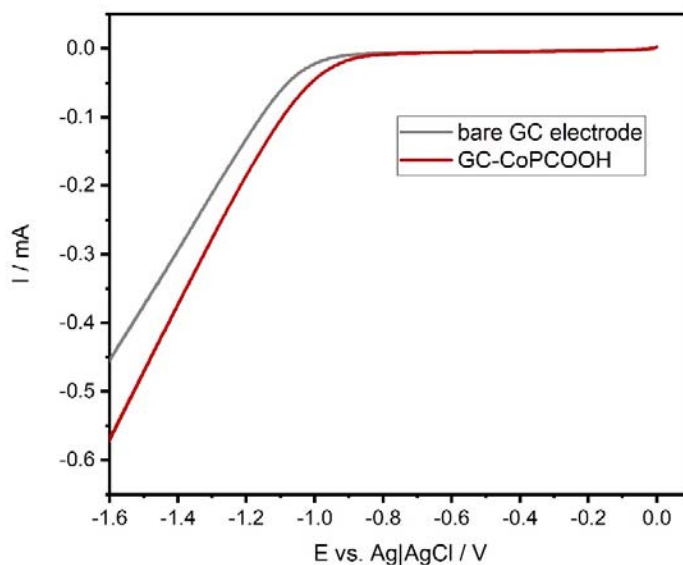


Figure S4. Catalytic response of CoPCOOH immobilized via drop-casting on a basal pyrolytic graphite (BPG) electrode, measured in buffer at pH 4 with a scan rate of 50 mV/s.

Cyclic voltammetry of CoPCOOH immobilized on a basal pyrolytic graphite electrode shows the catalytic activity towards hydrogen evolution reaction. The catalyst was loaded via dropping of 100 μ L of *ca.* 167 μ M concentrated catalyst solution. For the total amount of loaded catalyst on the surface, assuming 100 % Faradaic efficiency and unchanged activity of the BPG electrode, the averaged turnover frequency of the catalyst can be estimated according to the formula:

$$TOF = \frac{I_{GC+CoPCOOH} - I_{bare\ GC\ electrode}}{2nF}$$

Where n refers to number of moles of catalyst and F is the Faraday constant.

At an applied potential of -1.5 V the TOF of CoPCOOH yields a number of $0.03 \frac{1}{s}$.

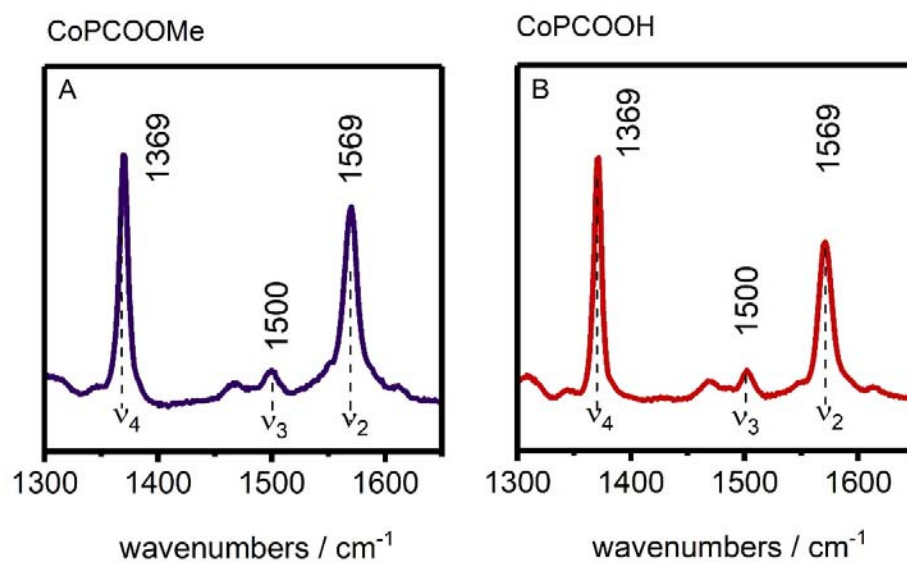


Figure S5. SERR spectra of (A) CoPCOOMe and (B) CoPCOOH immobilized on silver roughened electrodes, measured under open circuit conditions at pH 4. Dashed lines indicate positions of porphyrin vibrations.

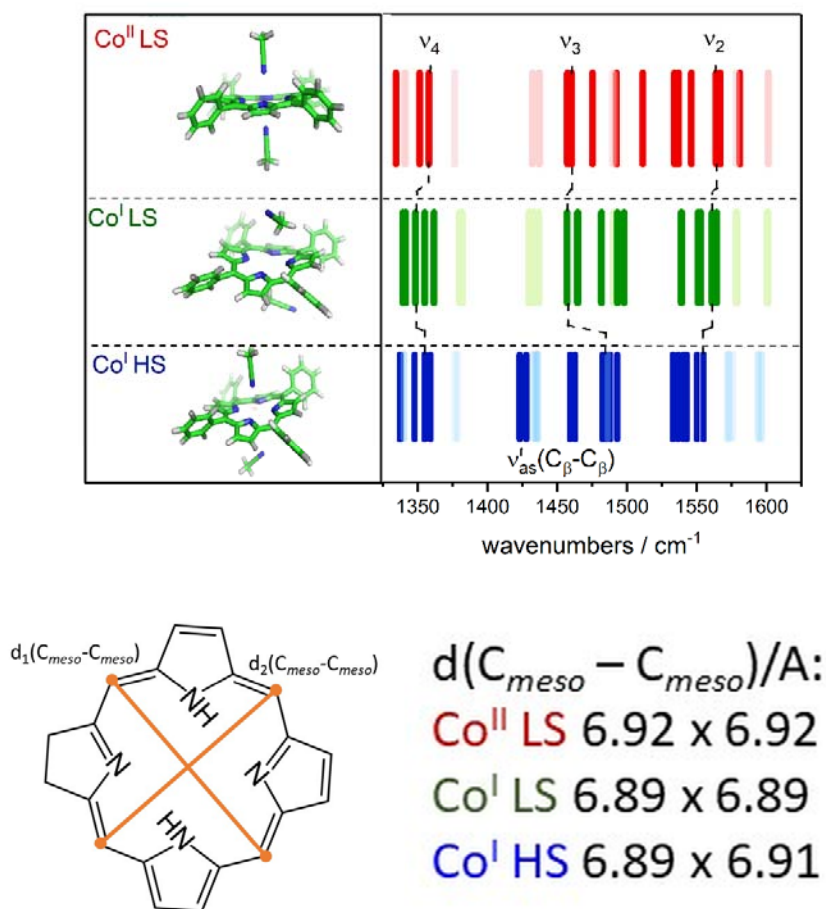


Figure S6. Top left: Optimized structures of CoTPP in the Co^{II} low-spin (LS), Co^I high spin (HS), and Co^I LS state, axially coordinated by two, one, and no acetonitrile molecules, respectively. Top right: Corresponding calculated vibrational frequencies. Porphyrin-centred normal modes are indicated by full-coloured lines, while normal modes dominated by vibrations of substituents at C_{meso} positions and acetonitrile molecules (non-enhanced modes) are depicted as light-coloured lines. Bottom: Calculated C_{meso}-C_{meso} distances of the above CoTPP species.

For a better understanding of experimental resonance Raman spectra, DFT calculations of CoTPP (cobalt tetraphenylporphyrin) in different oxidation states have been performed. As presented in Fig. S7, CoTPP in the Co^{II} LS state exhibits a *quasi* ideal planar porphyrin of approximate D_{4h} symmetry, with uniform C_{meso}-C_{meso} distances. The DFT-calculated vibrational “spectrum” of this state (Fig. S7, top) displays all modes, in contrast to experimental spectra, which show only the Raman-active and resonance-enhanced ones. Hence, characteristic totally symmetric porphyrin vibrations belonging to the A_{1g} symmetry group (v₄, v₃, v₂) could be assigned to the experimentally observable bands (full-coloured lines), while the other modes primarily reflect vibrations of the peripheral phenyl substituents of the porphyrin macrocycle and the coordinating acetonitrile molecules. In contrast to the oxidized form, the calculated structure of the Co^I state reveals a distortion of the porphyrin plane, irrespective of the spin state. The observed deviations from planarity can be best described as porphyrin “ruffling” and/or ‘saddling’, and the resulting structures could be assigned to the C_{4v} or S₄ point groups.^{2,3} In general, different features can lead to non-planar porphyrin deformations, namely large or small metal ions, bulky substituents, or axial coordination of the metal.^{3–6} At this stage, it is difficult to guess which of these factors dominates the observed porphyrin

distortions, and compensating influences of the xanthene linker, not included in the computational model, cannot be entirely excluded.

Due to non-planar porphyrin distortion, both Co^{I} HS and Co^{I} LS exhibit a lowered symmetry (*vide supra*). From this point of view, both species could be compatible with the (SE)RR-spectroscopic detection of a normal mode that is not expected to be observed for an idealized D_{4h} -symmetric porphyrin (Figs. 2CII, 2DII, 3C, and 3F). However, only Co^{I} HS exhibits a porphyrin-centred normal modes in the relevant spectral region between 1400 and 1450 cm^{-1} (Fig. S7, top right). Thus, we tentatively assign the experimentally observed state of reduced CoPCOOH and CoPCOOMe to the Co^{I} HS species. According to the calculations, atom displacements in the best candidate mode are dominated by a non-totally symmetric stretching of $\text{C}_{\beta}\text{--C}_{\beta}$ bonds, and, thus, it may be assigned to a ν_{11} -type B_{1g} -derived porphyrin vibration.⁷

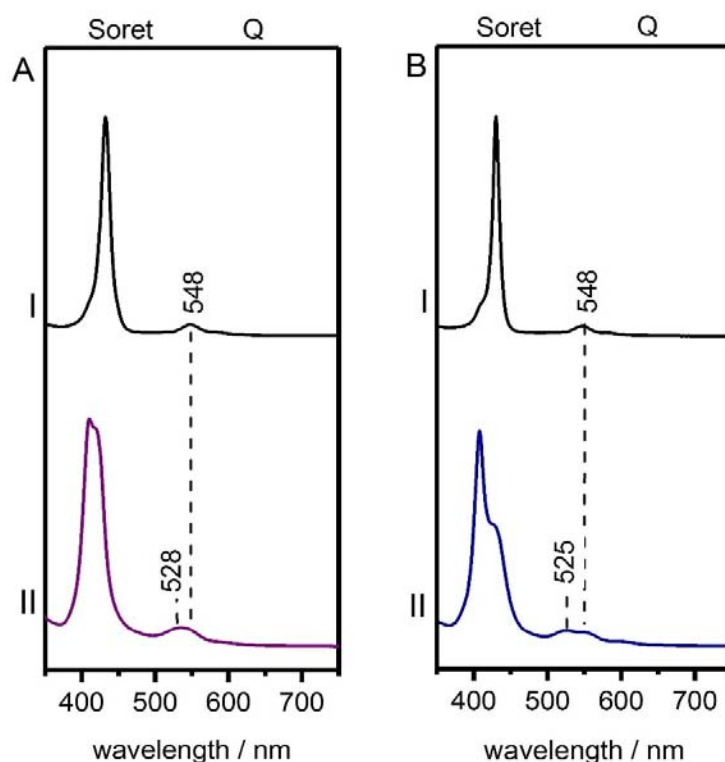


Figure S7. UV-Vis absorption spectra of (A) CoPCOOH and (B) CoPCOOMe dissolved in acetonitrile, in their (I) resting state and (II) after addition of KEt_3BH .

- 1 D. D. Bode, T. N. Andersen, and H. Eyring, *J. Phys. Chem.*, 1967, vol. 71, no. 4, pp. 792–797.
 - 2 P. M. Kozlowski, J. R. Bingham, and A. A. Jarzecki, *J. Phys. Chem. A*, 2008, vol. 112, no. 50, pp. 12781–12788.
 - 3 T. S. Rush, P. M. Kozlowski, C. a Piffat, R. Kumble, M. Z. Zgierski, and T. G. Spiro, *J. Phys. Chem. B*, 2000, vol. 104, no. 20, pp. 5020–5034.
 - 4 J. A. S. L. D. Sparks, C. J. Medforth, M. S. Park, J. R. Chamberlain, M. R. Ondrias, M. O. Senge, K. M. Smith, *J. Am. Chem. Soc.*, 1993, vol. 115, no. 2, pp. 581–592.
 - 5 J. A. Shelnutt, X. Song, J. Ma, S. Jia, W. Jentzen, C. J. Medforth, and C. J. Medforth, *Chem. Soc. Rev.*, 1998, vol. 27, no. 1, p. 31.
 - 6 C. Olea, J. Kuriyan, and M. A. Marletta, *J. Am. Chem. Soc.*, 2010, vol. 132, no. 37, pp. 12794–12795.
 - 7 R. A. Reed, R. Purrello, K. Prendergast, and T. G. Spiro, *J. Phys. Chem.*, 1991, vol. 95, no. 24, pp. 9720–9727.
-